ISSN 2063-5346

# STUDY OF MODIFIED COUNTER ELECTRODES USING NANOCOMPOSITE MATERIALS BASED ON REDUCED GRAPHENE OXIDE AS SEMI-TRANSPARENT FILM FOR PHOTOELECTROCHEMICAL SOLAR CELL.

**K. MEENA, R. K. BHUPESH, L. C. YADAV, V. SAINI, R. C. MEENA, and S. L. MEENA***

**Article History: Received: 10.05.2023 Revised: 29.05.2023 Accepted: 09.06.2023**

**Abstract**

This work creates semi-transparent composite film for photo electrochemical solar cell (PECSC) that used nanocomposite materials based on reduced graphene oxide as a counter electrode (CE) due to its high conductivity and electro catalytic activity. Platinum is too expensive and rare to use in PECSC.Graphite was transformed into graphene oxide using the Modified Hummer method and then chemically reduced. Variations in reduced graphene oxide dispersion in a number of organic solvents were seen using ultraviolet-visible spectroscopy. The PECSC counter electrodes were spin-coated using reduced graphene oxide, polyvinyl pyrrolidone, and poly(3,4-ethylenedioxythiophene)-poly(styrenesulfonate) composite film on fluorine-doped tin oxide (FTO) substrates. XRD and SEM techniques were used to characterise the semi-transparent film of counter electrode. It has been demonstrated that PECSC with counter electrodes made of reduced graphene oxide based nanocomposite can be used in solar cell applications.

**Keyword**: Solar cell, reduced Graphene oxide, Dispersed solution, Counter electrode.

Department of Chemistry, Jai Narain Vyas University, New Campus, Jodhpur, 342011, India

*Corresponding author: E-mail: slmeena.jnvu@gmail.com

**DOI:10.48047/ecb/2023.12.9.06**

## INTRODUCTION

Traditional fossil energy sources cannot support human civilization due to rising energy use and pollution [1]. Human civilization requires clean, renewable energy. Solar power is a potential new energy technology [2]. Sunlight is the source of solar energy. On Earth, it creates 1.4x $10^5$ TW. There is only 3.6 x $10^4$ TW of usable energy available [3]. Alternative energy sources include solar energy, globally accessible. Energy is generated without combustion [4-6]. Recently developed technologies turn renewable incident solar energy into electricity. Photovoltaic or photochemical processes turn light into electrical energy in a solar cell [7].

Using the knowledge and resources of the semiconductor industry, photovoltaic solar cells with a junction between inorganic materials and solid state—mostly crystalline or amorphous silicon—dominate the market [8–11]. Nanocrystalline and conductive polymer photovoltaic cells have challenged this supremacy in recent years. New photovoltaic cells may be made cheaply using flexible or non-toxic materials like titanium oxide, used in paints, cosmetics, and health items. A photo-electrochemical cell may be created by substituting the semiconductor contact phase with the electrolyte-liquid or solid. Nanocrystalline material preparation and characterization have expanded these systems' possibilities. Photoelectrochemical solar cells employ dye and nanocrystalline semiconductor with a large energy gap to absorb light and separate charges [12-16]. Photo anode, counter electrode, and electrolyte are components of photo electrochemical solar cells. In photo electrochemical solar cells, the counter electrode catalyzes the reduction of the redox pair and regenerates the dye following an injection of electrons or a mass of holes in a material that transmits holes. Redox coupling is required to move electrons from the external circuit to the electrolyte. Platinum-coated conductive glass is the most often used counter electrode, even though the platinum layers are to blame for the high cost of manufacture. New anti-corrosive, low-cost materials that can manufacture photo electrochemical solar cells with high efficiency are needed [17-20].

In the past few decades, there has been a rapid development of carbon nanomaterials, and the discovery of graphene has become one of the major factors driving the nanotechnology forward. The IUPAC describes graphene, a single carbon layer of the graphite structure, as "A single carbon layer, describing its nature by analogy to a polycyclic aromatic hydrocarbon of quasi-infinite size" [21]. Carbon atoms that have undergone $sp^2$ hybridization are joined to form a two-dimensional honeycomb structure. In order to form -bonds, $2p_z$ orbitals that are parallel to neighboring carbon atoms overlap. These bonds result in the creation of an electron cloud. Graphene was found in 2004[22]. Electrical conductivity of 6000 s $cm^{-1}$, Young's modulus of 1.0 TPa, strength of 130 GPa, thermal conductivity of 5000 W $m^{-1}$ $K^{-1}$, electron mobility of 200,000 $cm^2$ $Vs^{-1}$, and optical transmittance of 98% are all characteristics of graphene.

As graphene oxide (GO), reduced graphene oxide (rGO), and pristine graphene (G), there are three distinct forms of graphene. However, the name for graphene and its constituents is varied. Although Bianco et al. provided a formal nomenclature, it is not often used, therefore results must be carefully interpreted [23]. Graphite is oxidized to create GO, which is easily exfoliated [24] but has a very different composition from G [25]. Finally, GO may be reduced chemically or thermally to produce rGO [26]. A unique carbon-based nanoscale substance called reduced graphene oxide (GO) offers an alternative method of using

graphene. Due to reduced graphene oxide's solubility in water and other solvents, thin films or networks may be reliably produced on a range of substrates [27]. Because of this, it could be appropriate for microelectronics. Reduced graphene oxide dispersion is a black, aqueous liquid. Preparing a stable, highly concentrated reduced graphene oxide solution without surfactants or dispersants is difficult due to its hydrophobicity. Conductive films are formed by coating insulating surfaces with aqueous reduced graphene oxide. Energy barriers prevent agglomeration and maintain dispersion. Electrostatic or steric repulsion may do this [28]. The dispersion is maintained via Brownian motion when the energy barrier is strong [29]. This might be accomplished by choosing the right solvent [30] or by covalently or non-covalently altering reduced graphene oxide [31]. This could facilitate the production of hybrid or graphene-polymer composite materials [32-34]. In present study many solvents, as-prepared rGO produces stable dispersions solution by Ultrasonication process. On semi-transparent conductive oxide-coated glass, chemically reduced graphene oxide was explored examining counter electrodes. As counter electrodes for PEC solar cells, we can employ FTO-rGO nanocomposites to increase current density in comparison to pure FTO, hence improving power conversion efficiency. Therefore, low-cost spin coating of highly transparent homogenous nanocomposite thin films use as the counter electrode for PEC solar cells is technologically vital for green cost-effective efficient energy devices.

## EXPERIMENTAL

### Materials:

In this work, the fabrication of a few layers of graphene oxide (FLGO) was scaled up using graphite powder (Merck), 98 weight percent $H_2SO_4$, $KMnO_4$, $NaNO_3$, deionized water, $NH_3.H_2O$ aqueous, diluted HCl aqueous, 30% $H_2O_2$ aqueous, and 80% hydrazine hydrate aqueous all chemical is Loba Chemie and ASES Chemical. Bath sonication is used to uniformly distribute reduced graphene oxide (rGO) nanoparticle, PVP (Loba chemie), and PEDOT: PSS (Sigma Aldrich) in various solvents before they are mixed to form a slurry. Cut into 1×1 $cm^2$ pieces, FTO glass substrates (7Ω/sq, sigma) ultrasonically cleaned (PSAW, India) in distilled water, acetone, and ethanol for 15 minutes.

### Methods:

**Study in modified Hummers Methods for Graphite-to-Graphite Oxide/Graphite Oxide-to-reduced Graphene Oxide:** The standard experiment included dispersing 20 grams of graphite powder (Merck) in 450 ml of concentrated $H_2SO_4$ in a 5L beaker. $NaNO_3$ (15 grams) was added and stirred. Since the reaction is highly exothermic, it was placed in an ice bath and agitated with a stirrer that was coated with Teflon to maintain a temperature of less than 5 °C. 80 grams of Merck $KMnO_4$ powder were added while stirring. The reaction mixture was agitated after $KMnO_4$ was added. After 18 hours, the reaction mixture was brownish-gray slowly adding 1000 ml of deionized water to the reaction vessel brought the temperature up to 90 °C. Deionized water was used to dilute the reaction. The $MnO_4^-$ and $MnO_2$ were then converted into soluble $Mn^{2+}$ by the addition of 20 ml of 6% $H_2O_2$. The dark solution was vacuum filtered, rinsed with diluted $HNO_3$, and dried at 50 °C. Graphene-based nanocomposites were created using graphite oxide as a precursor. Graphite oxide was first made into a stable colloidal dispersion, and then it was reduced using hydrazine hydrate [35-36].

**Preparation of Reduced graphene oxide (rGO) dispersion solution:** The dried product underwent grinding in a mortar and pestle, followed by its combination with the solvent. To

create reduced graphene oxide dispersions, the mixture was then subjected to ultrasonic treatment in an ultrasonic bath cleaner for one hour. To investigate the dispersion behavior of various solvents, the nominal concentration was established at 0.5 mg $mL^{-1}$ by introducing 5 mg of reduced graphene oxide powder to 10 mL of solvent. The assessment of reduced graphene oxide dispersions encompassed acetone, 2-propanol, ethylene glycol, and NMP. All solvents contained less than 0.1% deionized water. As de-ionized water is typically used as a solvent for dispersions, aqueous dispersions of our prepared reduced graphene oxide material were created using the same methodology as the organic solvents, thereby contrasting the dispersions of organic solvents with those of deionized water [37].

**Preparation of rGO/PVP/PEDOT: PSSCounter Electrode:** We created rGO thin films on fluorine-doped tin oxide (FTO) substrates using commercial rGO powder dispersed in deionized water (DI Water) (0.5 mg $mL^{-1}$) at a predetermined ratio. Probe-type ultrasonication was employed for a uniform aqueous solution for a period of one hour. An electrode slurry was created by adding PVP (Polyvinyl Pyrrolidone) (0.05 gram) and PEDOT: PSS to the aqueous solution and stirring and homogenizing it magnetically for 5 hours. For one minute, GO suspension was spin coated at 3000 rpm. By employing ultrasonication, the fluorine-doped tin oxide (FTO) substrate was subjected to a thorough cleaning process using acetone, ethanol, and deionized water, each for a duration of 10 minutes. Subsequently, the FTO substrate was left to dry at room temperature for a period of 24 hours. Fig. 1. presents the observation of rGO thin films after the aforementioned drying period.

**Preparation of rGO/PEDOT: PSSCounter Electrode:** We create GO from graphite flakes using the Hummers Method, then using chemicals, we turn GO into rGO. Reduced graphene oxide counter electrode production is show in Fig. 1. An electrode slurry was created using a combination of PEDOT: PSS solution (3.0-4.0% in $H_2O$), reduced graphene oxide dispersion in deionized water (0.5 mg $mL^{-1}$), ultrasonication, magnetic stirring, and homogenization. PEDOT: PSS improved film formation and conductivity. On an FTO glass substrate, mixtures were deposited after a one-minute spin coating at 3000 rpm. At room temperature, the GO counter electrodes were vacuum-dried [38-47]. Prior to deposition, FTO glasses were ultrasonically cleaned for 15 minutes in deionized water, acetone, ethanol, and isopropanol. Reduced graphene oxide thin films are shown on different substrates in Fig. 2.

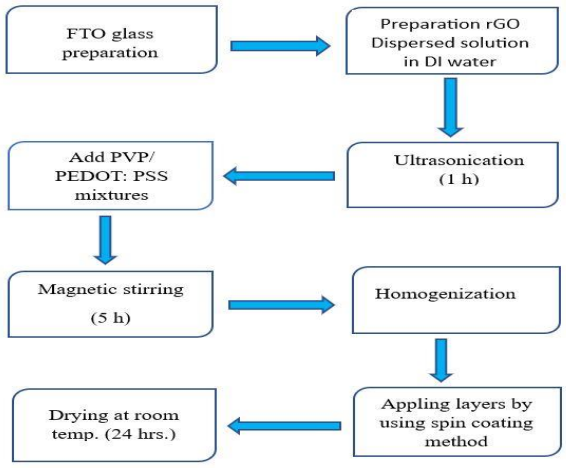


Fig.1. Production steps of counter electrodes

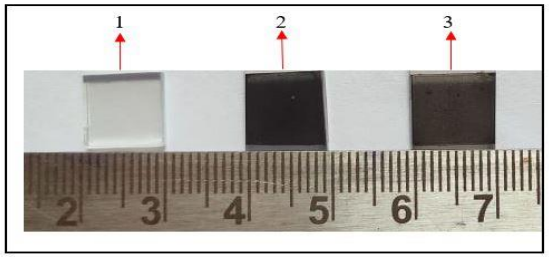


Fig. 2. Reduced Graphene Oxide thin films with different substrates (1) Blank-FTO (2) rGO/PVP/PEDOT: PSS-FTO (3) rGO/PEDOT: PSS-FTO

UV-visible spectra were recorded using the Systronics PC Based Double Beam spectrophotometer 2202 instrument. To facilitate qualitative comparisons among the various solvents, the UV-vis spectra were obtained under comparable conditions. Specifically, the spectra were captured two weeks after the dispersions achieved stability and were taken from dispersions that underwent equal dilution. (SEM) studies were carried out using SEM -Nova Nano FESEM 450 BY FEI for these samples were spread on to FTO substrate including rGO/PVP/PEDOT: PSS and rGO/PEDOT: PSS composite films by spin coated. XRD spectra of the nanocomposites were carried out using an XRD- Malvern Panalytical Xpert Powder to investigate the crystalline phases present in the samples (rGO/PVP/PEDOT: PSS, rGO/PEDOT: PSS).

## RESULTS AND DISCUSSION

**Reduced Graphene Oxide Dispersions:** As mentioned in the Experimental Section, the utilization of dispersed reduced graphene oxide is instrumental in attaining stability for flexible electronics. Once the stability threshold is rapidly achieved, numerous solvents become soluble. To achieve this, the as-prepared reduced graphene oxide material was dispersed in deionized water and four organic solvents using bath ultrasonication. The dispersion was carried out at a nominal concentration of 0.5 mg/mL, and the samples were left to settle for several weeks. Fig. 3 showcases all the dispersions, depicting their initial state after sonication as well as their appearance two weeks later.

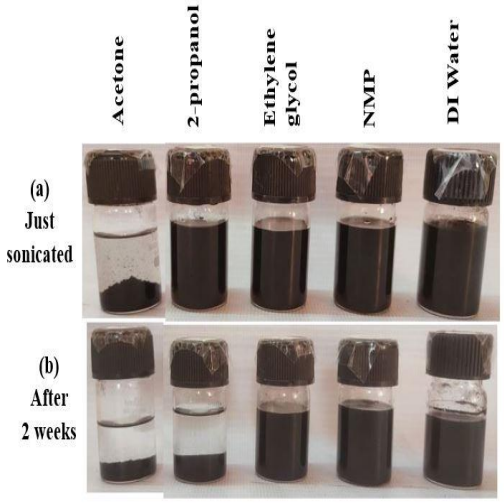


Fig. 3. rGO was dispersed in five different organic solvents using bath ultrasonication for one hour. Dispersions solutions just after sonication (a) at the top. (b) Bottom: solutions after two weeks for dispersions.

The sonicated samples exhibited the ability to disperse reduced graphene oxide in nearly all solvents, although many of these dispersions demonstrated only short-term stability and precipitated completely within a few hours to a few days. This was particularly observed in the case of 2-propanol and acetone. However, it was found that the long-term stability of reduced graphene oxide dispersions in two organic solvents, namely ethylene glycol and NMP, was comparable to that in de-ionized water. After the initial few days of sonication, only a small amount of precipitate was observed in the de-ionized water and the two aforementioned organic solvents, with no further precipitation occurring thereafter. This phenomenon was attributed to reduced graphene oxide material that could not be adequately exfoliated during the 1-hour sonication period. In fact, longer sonication times tended to decrease the amount of precipitate. Notably, ethylene glycol dispersions produced slightly more precipitate compared to de-ionized water and NMP dispersions under the same preparation conditions, indicating that the former solvents had a relatively lower dispersing capability. Fig. 4 shows the

UV-vis absorption spectra for the five stable reduced graphene oxide dispersions in acetone, deionized water, ethylene glycol, NMP, and 2-propanol. Additionally, the spectrum for the lowest concentration dispersion in acetone is included for reference.

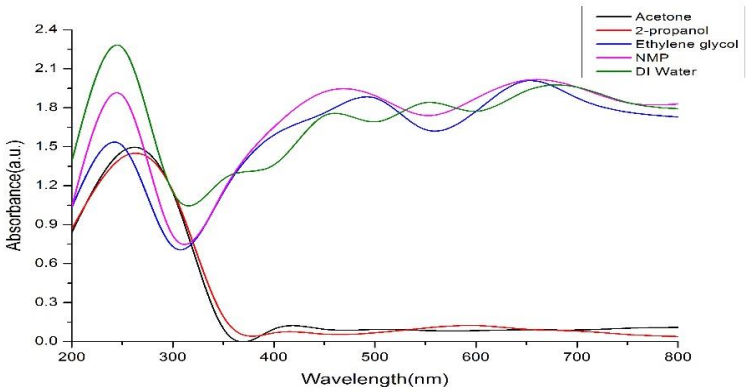


Fig. 4. UV-vis absorption spectra of reduced graphene oxide in various solvents.

The spectra were taken for stable dispersions, or those that had been prepared for two weeks. The dispersion solutions of r-GO in each solvent were assessed utilizing the Lambert-Beer equation, which establishes a linear relationship between absorbance (A) and concentration (C) of a molecule in a solution ($A = \alpha l C$). To determine the absorption coefficient ($\alpha$), representing the absorbance per unit path length (A/l), it was essential to define the dispersion characteristics. The data were observed at 250 nm due to the limited capability to account for significant absorption by the solvents at shorter wavelengths. The spectra encompassed the range of 200-800 nm. Based on the spectra obtained from different solvents, it was evident that the reduced graphene oxide material exhibited good dispersion in water, ethylene glycol, and NMP. The absence of absorption in acetone supported the previous finding that reduced graphene oxide dispersions in this solvent were unstable. Among the five effective solvents, water displayed the most favourable dispersion properties, as illustrated in Fig.4. This was attributed to water exhibiting the highest absorption intensity, resulting in the highest amount of suspended reduced graphene oxide. Ethylene glycol and NMP demonstrated remarkably similar dispersion characteristics for reduced graphene oxide. The maximum solubility of GO and rGO in each solvent was determined (Table-1) [45].

TABLE-1

The Values of all Solvents (Dipole moment, Surface Tension and Graphene oxide, reduced graphene oxide Solubility)

| Solvents | Dipole moment | Surface tension (mN/m) | GO Solubility (µg/mL) | rGO Solubility (µg/mL) |
|---|---|---|---|---|
| Di water | 1.85 | 72.8 | 6.6 | 4.74 |
| Acetone | 2.88 | 25.2 | 0.8 | 0.9 |
| 2-propanol | 1.66 | 21.66 | 1.82 | 1.2 |
| Ethylene glycol | 2.31 | 47.7 | 5.5 | 4.9 |
| N-methyl-2-pyrrolidone (NMP) | 3.75 | 40.1 | 8.7 | 9.4 |

**Scanning Electron Microscope Study**: SEM micrographs of Fig. 5 show a range of counter electrodes, including rGO/PVP/PEDOT: PSS and rGO/PEDOT: PSS composite films coated on FTO substrate. because rGO has less oxygen functional groups. In light of the results, we only used DI water as the rGO dispersion medium. During the spin coating process, the rGO sheets were flattened and evenly distributed across the PEDOT: PSS matrix. It is clear in both the pictures that the surface morphology of the second electrode is better than that of the first electrode because poly vinyl pyrrolidine is abinder used in the first electrode, which is not a good binder, so the morphology of the second electrode is better. PEDOT: PSS was employed to improve film forming capacity and conductivity. Show in fig.5. Sample (1) rGO/PVP/PEDOT: PSS FTO, SEM images of certain counter electrodes were captured and sample (2) rGO/PEDOT: PSS FTO glass slide coated layer is visible at various magnifications, including (a) 100,000x, (b) 50,000x and (c) 100,000x, (d) 50,000x

**X –Ray Diffraction Study:** Lattice and molecular structure of a chemical (in thin film form) are determined using XRD. These particles become diffuse when an x-ray beam strikes them in all directions. The electron density inside a crystal lattice is represented in three dimensions by XRD using intensity and scattering ray angle data. Without causing any harm to the sample, XRD uses Bragg's law ($n\lambda=2D \sin\theta$) as its basic guiding principle. To comprehend the crystal phase and establish the interlayer gap, XRD experiments were conducted. Fig. 6 displays the XRD spectra of two different thin films made of rGO/PVP/PEDOT: PSS, respectively. One distinct peak can be seen in spectrum (a) at a $2\theta$ angle of 26.59. The existence of a layer structure with 3.35287 d-spacing (FWHM = 0.1378) was verified by this peak. Another peak may be seen at the following $2\theta$ angles: 33.80°, 37.79°, 51.53°, 54.72°, 61.58°, 65.55°, and 78.34°; the corresponding d-spacing for each is 2.65205, 2.38073, 1.67750, 1.50604, 1.42410, and 1.22053°. A strong peak in spectrum (b) may also be seen at a $2\theta$ angle of 26.58. With a 3.35360 d-spacing (FWHM = 0.1574), this peak demonstrated the existence of a well-organized layer structure. Another peak is seen at the following $2\theta$ angles: 33.76°, 37.82°, 51.49°, 54.60°, 61.63°, 65.53°, and 78.33°; the corresponding d-spacing is: 2.65479°, 2.37878°, 1.77488°, 1.50498°, 1.42448°, and 1.22065°. During the chemical reduction, the functional groups containing oxygen were drastically reduced. This shows that at the generated rGO, graphene's -conjugated structure has been significantly restored. It also showed that the presence of strong van der Wall forces between each layer caused the thin rGO nanosheet to be layered on top of one another to create a thick pile.

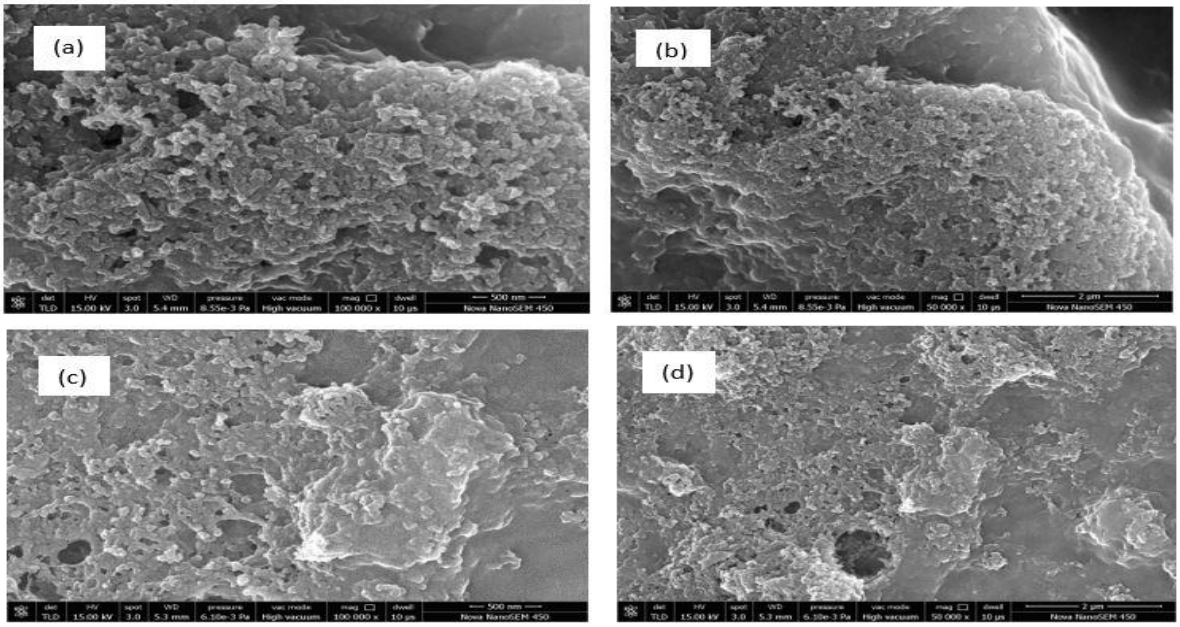


Fig.5. SEM micrographs of sample (1) rGO/PVP/PEDOT: PSS FTO glass slide coated layer shows at various magnifications (a) 100,000 x (b) 50,000 x and sample (2) rGO/PEDOT: PSS FTO glass slide coated layer shows at different magnifications (c) 100,000 x (d) 50,000 x

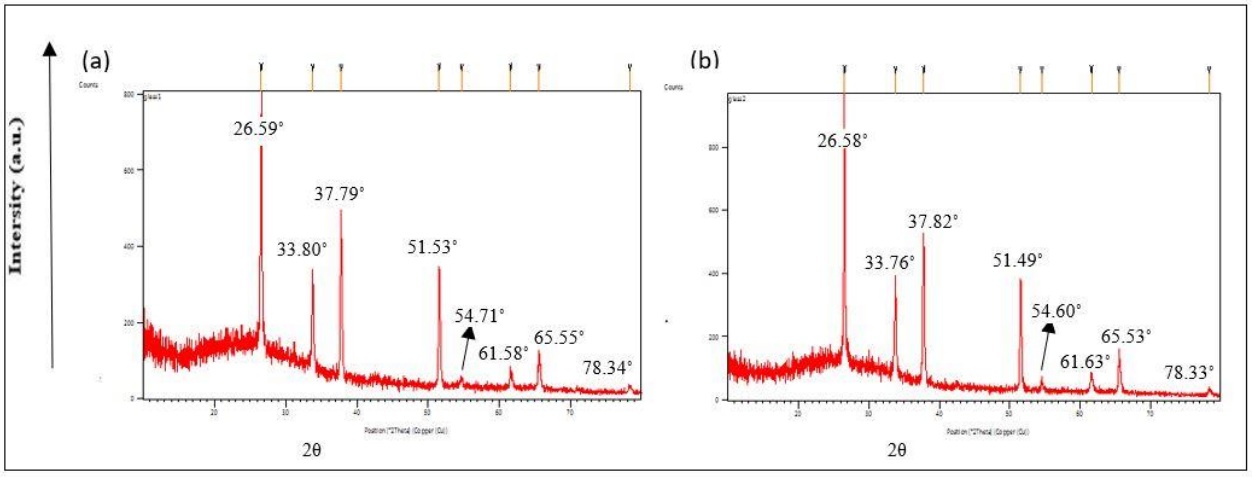


Fig.6. XRD spectra of (a)rGO/PVP/PEDOT: PSS nanocomposite thin film and (b) rGO/PEDOT: PSS nanocomposite thin film

## CONCLUSION

Reduced graphene oxide is a novel counter electrode material for the creation of high-performance, low-cost photo electrochemical solar cells/DSSC due to its adaptable structure, exceptional conductivity, and great film-flexibility. We have found a number of organic solvents where reduced graphene oxide may produce stable dispersions over the long term. As a result, these dispersions are analogous to the reduced graphene oxide dispersions in Di- water that are presently utilized to make various reduced graphene-based products, which should make it easier to process and further develop these materials. This dispersion technique offers a straightforward and cost-effective method for producing reduced graphene oxide for a variety of technological applications, such as graphene-based composites materials electrodes for solar cells. We have achieved the successful

fabrication of r-GO transparent composite thin films on FTO substrate using a spin coater. The successful fabrication of both electrodes of the r-GO was characterization by XRD and SEM techniques. We can successfully utilize of counter electrodein dye-sensitized solar cells, lithium-ion and sodium-ion batteries, super capacitors environmental and photo-catalytic applications. Therefore, much future study is required to have a better understanding the function of nanocomposite Materials based on reduced graphene oxide use as counter electrodes in solar cell.

## ACKNOWLEDGEMENTS

Financial support from University Grant Commission (UGC) -Junior Research Fellowship (Ref. No.: 140/ (CSIR-UGC NET DEC. 2017)) to one of the author (Kavita Meena) and during research others authors are highly acknowledged. Thanks are also due to Department of Chemistry, J.N.V. University, Jodhpur, Malaviya National Institute of Technology (MNIT), Jaipur and Scientium Analyze Solution (SAS), Jaipur, India for characterization facility.

## CONFLICT OF INTEREST

The authors declare that there is no conflict of interests regarding the publication of this article.

## REFERENCES

1. A. Louwen, W.G.J.H.M.V. Sark, A.P.C. Faaij and R.E.I. Schropp, *Nat Commun.*, **7**, 13728 (2016); https://doi.org/10.1038/ ncomms13728
2. V. Ooteghem, R. J.C., *IFAC Proceeding*, **43**, pp. 304–309 (2010); doi:10.3182/20101206-3-jp-3009.00054
3. R.H.E. Hassanien, M. Li, F. Yin, *Renew. Energy*, **121**, pp. 377–388 (2018);https://doi.org/10.1016/J.RENENE.2018.01.044
4. M. Hosenuzzaman, N.A. Rahim, J. Selvaraj, M. Hasanuzzaman, A.B.M.A. Malek, A. Nahar, *Renew. Sustain. Energy Rev.*, **41**, pp. 284–297 (2015);https://doi.org/10.1016/J.RSER.2014.08.046
5. E. Kabir, S. Kumar, P. Kumar, A.A. Adelodun, K.H. Kim, *Renew. Sustain. Energy Rev.*, **82**, pp. 894–900 (2018); https://doi.org/10.1016/J.RSER.2017.09.094
6. N. Roslan, M.E. Ya'acob, M.A.M. Radzi, Y. Hashimoto, D. Jamaludin, G. Chen, *Renew. Sustain. Energy Rev.*, **92**, 171–186 (2018); https://doi.org/10.1016/J.RSER.2018.04.095
7. N.A. Karim, U. Mehmood, H. F. Zahid, T. Asif, *Solar Energy*, **185**, pp. 165–188 (2019);doi:10.1016/j.solener.2019.04.057
8. M. Musztyfaga-Staszuk, L.A. Dobrzański, *Central European Journal of Physics*, **12**, pp. 836-841 (2014); https://doi.org/10.2478/s11534-014-0512-5
9. M. Musztyfaga, L.A. Dobrzański, S. Rusz, M. Staszuk, *Archives of Metallurgy and Materials*,**59**, pp. 247-252 (2014); DOI:10.2478/amm-2014-0040
10. L.A. Dobrzański, M. Giedroć, A. Drygała, *Archives of Materials Science and Engineering*, 102, pp. 59-85 (2020); DOI:10.5604/01.3001.0014.1525
11. M. Grätzel, *Journal of Photochemistry and Photobiology C: Photochemistry Reviews*, **4** pp. 145-153 (2003); https://doi.org/10.1016/S1389-5567(03)00026-1
12. S. Stankovich, D.A. Dikin, R.D. Piner, K.A. Kohlhaas, A. Kleinhammes, Y. Jia, Y. Wu, S.T. Nguyen, R.S. Ruoff, *Carbon*, **45**, pp. 1558–1565 (2007);https://doi.org/10.1016/j.carbon.2007.02.034

13. J. Gong, J. Liang, K. Sumathy, *Renewable and Sustainable Energy Reviews*, **16**, pp. 5848-5860 (2012); https://doi.org/10.1016/j.rser.2012.04.044
14. A. Yella, H-W. Lee, H.N. Tsao, C. Yi, A.K. Chandiran, M.K. Nazeeruddin, E.W-G. Diau, C.Y. Yeh, S.M. Nazeeruffin, M. Gratzel, *Science*, **334**, pp. 629-634 (2011); DOI: 10.1126/science.1209688
15. W. Shu, Y. Liu, Z. Peng, K. Chen, C. Zhang, W. Chen, *Journal of Alloys and Compounds*, **563**, pp. 229-233 (2013); https://doi.org/10.1016/j.jallcom.2013.02.086
16. K. Nazeeruddin, R. Splivallo, P. Liska, P. Comte, M. Grätzel, *Chemical Communications*, **12**, pp. 1456-1457 (2013); https://doi.org/10.1039/C3CC90019C
17. S. Sheehan, P.K. Surolia, O. Byrne, S. Garner, P. Cimo, X. Li, *Solar Energy Materials & Solar Cells*, **132**, pp. 237-244 (2015); https://doi.org/10.1016/j.solmat.2014.09.001
18. S. Kambe, S. Nakade, T. Kitamura, Y. Wada and S. Yanagida, *J. Phys. Chem. B*, **106**, 2967 (2002); https://doi.org/10.1021/jp013397h
19. Y. Yang, B. Maeng, D.G. Jung, J. Lee, Y. Kim, J.B. Kwon, H.K, An, D. Jung, *Nanomaterials*, **12**, 3227 (2022); https://doi.org/10.3390/nano12183227
20. M. Coroş, F. Pogăcean, L. Măgeruşan, C. Socaci, S. Prunenu, *Front. Mater. Sci.*, **13**, pp. 23–32 (2019); https://doi.org/10.1007/s11706-019-0452-5
21. A. K.Geim,K.S. Novoselov, *Nature Mater.*, **6**, 183 (2007);https://doi.org/10.1038/nmat1849
22. K. S. Novoselov, *Science*, **306**, pp. 666–669 (2004); DOI: 10.1126/science.1102896
23. A. Bianco, H.M. Cheng, T. Enoki, Y. Gogotsi, R.H. Hurt, N. Koratkar, T. Kyotani, M. Monthioux, C.R. Park, J.M. Tascon, J. Zhang, *Carbon*, **65**, pp. 1–6 (2013); https://doi.org/10.1016/j.carbon.2013.08.038
24. Y. Hernandez, M. Lotya, D. Rickard, S.D. Bergin, J.N. Coleman, *Langmuir*,**26**, pp. 3208–3213 (2010); https://doi.org/10.1021/la903188a
25. M.M. Gudarzi, M.H.M. Moghadam, F. Sharif, *Carbon*, **64**, pp. 403–15 (2013);https://doi.org/10.1016/j.carbon.2013.07.093
26. Y. Zhu, S. Murali, W. Cai, X. Li, J.W. Suk, J.R. Potts, R.S. Ruoff, *Adv Mater*, 22, 3906-24 (2010); doi:10.1002/adma.201090011
27. S. Pei, H.M. Cheng, *Carbon*,**50**, pp. 3210–28 (2012);https://doi.org/10.1016/j.carbon.2011.11.010
28. Y. Shang, D. Zhang, Y. Liu, C. Guo, *Bull Mater Sci*, **38**, pp. 7–12 (2015); https://doi.org/10.1007/s12034-014-0794-7
29. B.J. Hong, O.C. Compton, S.T. Nguyen, *ACS Nano*, **6**, pp. 63–73 (2012); https://doi.org/10.1021/nn202355p
30. A.S. Wajid, S. Das,F.Irin, A.H.S. Tanvir, J.L. Sherlburne,D.Parviz, R.J. Fullerton, A.F. Jankowski, R.C. Hedden, M.J. Green, *Carbon*, **50**,pp.526-534 (2012);https://doi.org/10.1016/j.carbon.2011.09.008
31. M. Ayán-Varela, J.I. Paredes, S. Villar-Rodil, R. Rozada, A. Martínez-Alonso, J.M.D. Tascón, *Carbon*, **75**, pp. 390–400 (2014); https://doi.org/10.1016/j.carbon.2014.04.018
32. T. Kuila, S. Bose, A.S. Mishra, P. Khanra, N.H. Kim, J.H. Lee, *Prog Mater Sci*, **57**, pp. 1061–105 (2012); https://doi.org/10.1016/j.pmatsci.2012.03.002
33. S. Perumal, R. Atchudan, W. Cheong, *Polymers*, **13**, 2375 (2021); https://doi.org/10.3390/polym13142375

34. D.W. Johnson, B.P. Dobson, K.S. Coleman, *Current Opinion in Colloid & Interface, Science*,**20**, pp. 367–382 (2015); doi:10.1016/j.cocis.2015.11.004
35. L.A. Dobrzański, M. ProkopiukvelProkopowicz, K. Lukaszkowicz, A. Drygała, M. Szindler, *Journal of Achievements in Materials and Manufacturing Engineering*, **73**, pp. 13-20 (2015); DOI:10.1016/j.solener.2011.11.010
36. S.N. Tripathi, G.S.S. Rao, A.B. Mathur, R. Jasra, *RSC Adv.*, **7**, pp. 23615–23632 (2017);DOI: 10.1039/C6RA28392F
37. D. Konios, M.M. Stylianakis, E. Stratakis, E. Kymakis, *Journal of Colloid and Interface, Science*,**430**, pp. 118-120 (2014); http://dx.doi.org/10.1016/j.jcis.2014.05.033
38. H. Wang, K. Sun, F. Tao, D.J. Stacchiola, Y.H. Hu, *Angewandte Chemie International Edition*, **52**, pp. 9210-9214 (2013); https://doi.org/10.1002/anie.201303497
39. C.T. Hsieh, B.H. Yang, Y.F. Chen, *Diamond & Related Materials*,**27**, pp. 68-75 (2012);https://doi.org/10.1016/j.diamond.2012.06.002
40. D.W. Zhang, X.D. Li, H.B. Li, S. Chen, Z. Sun, X.J. Yin, S.M. Huang, *Carbon*, **49**, pp. 5382-5388 (2011); https://doi.org/10.1016/j.carbon.2011.08.005
41. H.S. Jang, J.M. Yun, D.Y Kim, D.W. Park, S.I. Na, S.S. Kim, *Electrochimica Acta*,**81**, pp. 301-307 (2012); https://doi.org/10.1016/j.electacta.2012.07.021
42. Z.Y. Li, M.S. Akhtar, J.H Kuk, B.S. Kong, O.B. Yang, *Material Letters*, **86**, pp. 96-99 (2012); https://doi.org/10.1016/j.matlet.2012.07.006
43. L. Wan, S. Wang, X, Wang, B. Dong, Z. Xu, X. Zhang, B. Yang, S. Peng, J. Wang, C. Xu, *Sold State Sciences*, **13**, pp. 468-475 (2011);https://doi.org/10.1016/j.solidstatesciences.2010.12.014
44. W. Hong, Y. Xu, G. Lu, C. Li, G. Shi, *Electrochemistry Communications*, **11**, pp. 1555-1558 (2008); https://doi.org/10.1016/j.elecom.2009.05.056
45. M. Zhu, X. Li, W. Liu, Y. Cui, *Journal of Power Sources*, **262**, pp. 349-355 (2014);https://doi.org/10.1016/j.jpowsour.2014.04.001
46. S. Satapathi, H.S. Gill, S. Das, L. Li, L. Samuelson, M.J. Green, J. Kumar, *Applied Surface Science*,**314**, pp. 638-641 (2014); https://doi.org/10.1016/j.apsusc.2014.07.003
47. X. Fang, M. Li, K. Guo, Y. Zhu, Z. Hu, X. Li, B. Chen, X. Zhao, *Acta*, **65**, pp. 174-178 (2012); https://doi.org/10.1016/j.electacta.2012.01.038